

# Conformal polishing approach: Tool footprint analysis

José A Dieste<sup>1</sup>, Angel Fernández-Cuello<sup>2</sup>, Carlos Javierre<sup>2</sup>  
and Jorge Santolaria<sup>3</sup>

## Abstract

Polishing process is one of the most critical manufacturing processes during a metal part production because it determines the final quality of the product. Free-form surface polishing is a handmade process with lots of rejected parts, scrap generation and time and energy consumption. Two different research lines are being developed: prediction models of the final surface quality parameters and an analysis of the amount of material removed depending on the polishing parameters to predict the tool footprint during the polishing task. This research lays the foundations for a future automatic conformal polishing system. It is based on rotational and translational tool with dry abrasive in the front mounted at the end of a robot. A tool to part concept is used, useful for large or heavy workpieces. Results are applied on different curved parts typically used in tooling industry, aeronautics or automotive. A mathematical model has been developed to predict the amount of material removed in function of polishing parameters. Model has been fitted for different abrasives and raw materials. Results have shown deviations under 20% that implies a reliable and controllable process. Smaller amount of material can be removed in controlled areas of a three-dimensional workpiece.

## Keywords

Finishing, polishing, robot polishing, conformal polishing, polishing model

Date received: 9 June 2015; accepted: 3 January 2016

Academic Editor: Yong Tao

## Introduction

Finishing processes as polishing are present in most of the manufacturing workflows for industrial parts. Polishing is still a handmade process that requires research and development to increase the quality and reliability, reduce the parts rejection or time–cost and reach the challenges described in the strategic research agendas of the factories of the future. Researchers have been sensible during the last years to this problem trying to solve it through different research strategies.

The chemical mechanical polishing (CMP) was developed during the last 20 years and has rapidly grown as a core technology in the manufacturing of semiconductor devices due to its excellent flattening capacity.<sup>1–4</sup> The CMP is based on a rotating table, a polishing head and a suspension pad, where the surface

of the wafer moves across the pad, under pressure, in the presence of slurry abrasive. The mechanical movement and the downward force are applied to the wafer by the machine. The surface of the pad provides the rough spots, or asperities, which contact the wafer. The liquid suspension provides the abrasive particles and the right chemistry for the CMP performing.

<sup>1</sup>R&D Department, Fundacion AITIIP, Zaragoza, Spain

<sup>2</sup>Mechanical Engineering Department, University of Zaragoza, Zaragoza, Spain

<sup>3</sup>Manufacturing Engineering Department, University of Zaragoza, Zaragoza, Spain

## Corresponding author:

Angel Fernández-Cuello, Mechanical Engineering Department, University of Zaragoza, c/María de Luna, 3, 50018 Zaragoza, Spain.

Email: angel.fernandez@unizar.es



Creative Commons CC-BY: This article is distributed under the terms of the Creative Commons Attribution 3.0 License

(<http://www.creativecommons.org/licenses/by/3.0/>) which permits any use, reproduction and distribution of the work without

further permission provided the original work is attributed as specified on the SAGE and Open Access pages (<https://us.sagepub.com/en-us/nam/open-access-at-sage>).

The use for semiconductor industry makes CMP broadly develop during the last years. Combination of electrochemical finishing and burnishing has shown successful results on bore surfaces.<sup>5</sup> This polishing process is an example of how technology evolves to new industry requirements. CMP process is used to planar surfaces but is not applicable to three-dimensional (3D) free-form shapes. Then a different process has to be used.

Automation of general polishing process is required to be used in different industrial sectors, such as aeronautics, automotive and tooling industry. Common characteristics to these industrial parts are that the main shapes are 3D free form. To finish these surfaces, CMP is not valid and the complexity of the geometrical surfaces leads finishing to be done manually.

This research is focused on a future automated method to polish metallic parts based on robotics. Industrial robot is a very flexible machine that allows a large possible poses range. This enables to process surfaces in a large workspace. Control systems permit to process them with the correct tool angle position. Advantages of a 6-degree of freedom (DOF) robot, compared with other machines used for polishing process, are mainly related to the low investment that robot purchase supposes in comparison with milling machines,<sup>6</sup> turning machines or special machines.<sup>7</sup>

Recently, some intends to develop an automated polishing system based on robotics. There are two main concepts that can be used. The most extended is a part to tool philosophy that consists in one robot that handles the part and makes it go against an abrasive belt.<sup>8,9</sup> This is used in general industry to finish lightweight metallic parts, but it is not useful for heavy weight parts, that are the main objective of this research. Ultraform finishing (UFF) is a set of different-sized five-axis CNC machines equipped with an abrasive belt. They are commercialised by Optipro.<sup>10-12</sup> Then for heavy parts, as aeronautic aluminium parts, aluminium and magnesium automotive parts, or moulds and tools for industry, a tool to part concept is going to be used. In this case, robot handles a rotational tool and describes polishing trajectories over the workpiece that remains fixed in the cell.

Computer-controlled polishing systems have been commercialised recently. Magneto-rheological finishing (MRF) was developed since the end of the 1990s,<sup>13,14</sup> and QED Technologies International, Inc offers different machines for optical applications with multi-axis CNC machine to polish parts up to 2.000-mm length. In the field of large optical parts, polishing Zeeko commercialises an intelligent robotic polishing (IRP) technology based on seven-axis CNC machine using abrasive suspended in a fluid.<sup>15,16</sup>

Researches to make this process automated should solve the problems that current manual polishing is

carrying on, which are derived of the control lack in the process. Manual polishing requires of expert operators with a large experience but final quality part depends on their skills. The human intervention in polishing shows the absence of repeatability and involves a lot of part rejection. Lack of control in the process can be divided in two essential lines:

- No control in the methodology that defines the final surface quality parameters as roughness and brightness. Although majority of the polishing operators have a lot of experience, tools, abrasives, movements and methodology differ in each case. This has an important influence in the final aspect of the part and the time consumption in the process. The operator itself fixes the quality threshold, so the final quality of the part does not depend on objective criteria.
- No control in the amount of removed material. Manual polishing consists in a fuzzy sequence of movements of the abrasive on the workpiece. The only intention is to remove the previous marks, so there is no control on the material that is removed in each area. It derives in a lack of geometrical control of the shape of the polished part. Over polishing derives in rejected parts due to the final shape does not fit the geometrical requirements that should be achieved. In the rest of the cases, warpage or deformations in the surfaces are generated during the manual polishing.

Previous research has been done in order to improve the state of the art in several fields related to finishing and polishing. Narayanasamy et al.<sup>17</sup> and Li et al.<sup>18</sup> analysed defects appearing on parts during grinding and polishing process and classified them. Sachtleber et al.<sup>19</sup> and Xhang et al.<sup>20</sup> studied the physic phenomena that involved some of the defects as colour changes and hardening.

Several investigations focused on automation with industrial robots to analyse the influence of robotic paths on the results.<sup>21-25</sup> In this line, Huissonn et al.,<sup>26</sup> Pessoles and Tournier,<sup>27</sup> Feng et al.<sup>28</sup> and Tsai et al.<sup>29,30</sup> have shown that industrial trials were made for specific industrial sectors such as tooling industry.

This research has been performed in order to control the roughness of the part during automated polishing processes that is one of the goals to be achieved.

In this research, material removed by the tool has been analysed for a tool to part robotic polishing process.

Regarding material removal, some modifications based on Preston equation has been studied, Maury et al.,<sup>31</sup> for CMP.<sup>32-36</sup> Even some pure mechanical polishing processes have been modelled analysing contact stress<sup>37</sup> and influence of parameters on processing time.<sup>38</sup>

In the case of pure mechanical polishing that is the focus of this article, some mathematical models were done by Tam and Cheng<sup>39</sup> to analyse the final surface aspect in function of the typology of the polishing paths used.

During this research, a new model has been developed to predict tool footprint for a rotational sandwich tool. In addition, it has been determined how technological polishing parameters affect the amount of material removed and the final geometrical shape of the part. This model has been developed for a wide range of abrasives and has been tested in several materials.

The large control on the prediction obtained permits to open new research lines to achieve a conformal polishing process.

## Materials and methods

### Materials and installation

This investigation is based on a robotic system. Several machines such as milling machines were compared to perform polishing task in industrial environment. Due to the movement flexibility, the small maintenance and relative low investment, an industrial-size conventional robot KUKA KRC60 HA (Figure 1) was adapted and installed to perform polishing task in an automated way.

Robot controller is connected with an external PC where computer-aided manufacturing (CAM) software is running. In this case, CAM software is used to make an off-line programming of the robot trajectories,



**Figure 1.** Finishing robotic cell and grinding and polishing tool.

movements and poses to move the tool to polish the part. Delcam's PowerMill is the software used.

Some previous research uses rigid tool to perform polishing tasks on free-form surfaces. In these cases, surfaces of revolution such as cylinders or spheres are polished as it is required that finishing tool geometry fits exactly the shape of the part.<sup>40</sup> Free-form surfaces or complex geometries require the use of a force control system.<sup>41</sup> Research about process control,<sup>42</sup> force control<sup>43,44</sup> and compensating error due to machine force<sup>45</sup> has been developed recently for aspheric surfaces. The intention is to control the force that the tool is applying to the part during the finishing task. This system concept is probed valid for flat or planar surfaces, but in the case of convex or concave surfaces, new problems appear.<sup>46</sup> When a constant force is applied to the tool over polishing appear in convex areas while a lack of polishing affect the concave ones, so that constant force control can be applied only if tool shape fits with workpiece surface.<sup>47</sup>

To overcome the problem, a new tool is used<sup>46,48</sup> in this research. This tool maintains the nearest constant pressure in the contact surface between the tool and the workpiece. The design consists in a multilayer system comprising an abrasive layer assembled on the top of a urethane closed pore foam layer, which is mounted over a rigid metallic support. In this research, a rotating 30-mm-diameter tool with a 5-mm-thickness urethane core is used. It generates uniform contact pressure for thickness compression in the range of 10%–50% of the core. Non-flat, large curvature radius surfaces were successfully polished.

### Probes and test configuration

Investigation performed by Preston showed that the rate of material removed during polishing processes depends on the materials, the contact force and the relative velocity. As the objective of this research is to apply a constant pressure, the test trajectories are programmed to perform interference between abrasive and workpiece of 40% of the urethane foam layer thickness. Material for initial probes is aluminium 5083, and parameters obtained will be extrapolated and tested for magnesium and steel F114.

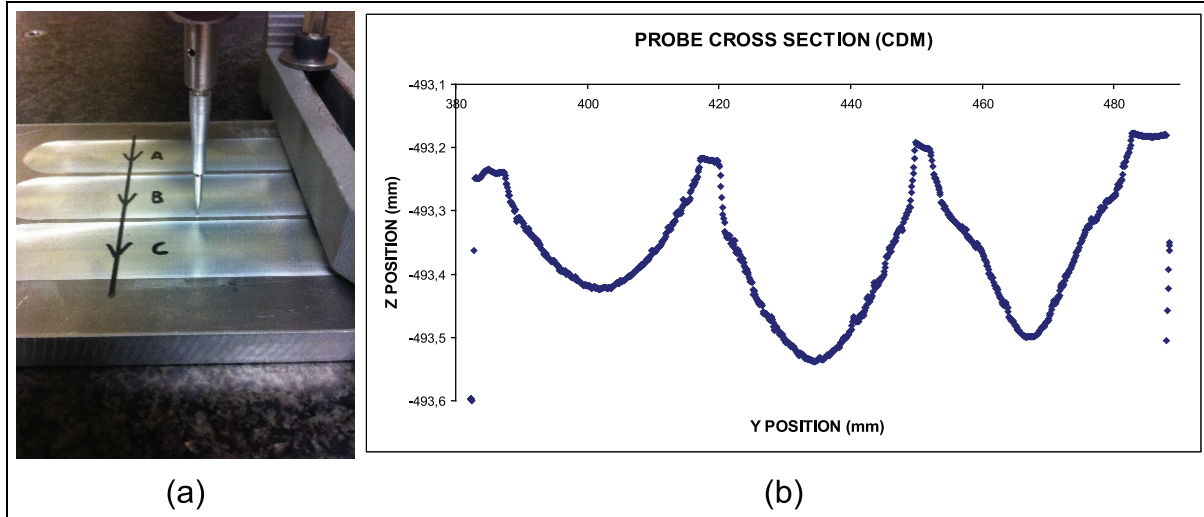
Because of the nature of polishing process, the surface states are obtained as a sequence of material removing operations. For this reason, the use of a roughness evolution model is needed.

Polishing is a multistep process that uses abrasive to remove material, this concept is translated in the use of a grain abrasive sequence, that is starting on a rough abrasive (large grain size) till a soft abrasive (small grain size).

In this research, the abrasive sequence is not crucial, as tool footprint is going to be analysed for a single

**Table 1.** Abrasive codes and mean grain size diameter.<sup>49,50</sup>

Abrasive code	F80	F120	F220	F400
Mean grain size ( $\mu\text{m}$ )	185	109	58	17.3

**Figure 2.** (a) Measuring process and (b) dimensional results of the tool footprint.

abrasive separately. Abrasives used are shown in Table 1. The values of mean grain sizes are extracted from FEPA-Standard 42-1:2006<sup>49</sup> and standard ISO 8486<sup>50</sup> and have a tolerance of  $\pm 20\%$ .

For each abrasive, it is necessary to determine the evolution curve.<sup>21,51</sup> To analyse the evolution curve, a series of trials have been performed for each abrasive. Once parameters related to pressure and material are fixed, the main parameters that will influence the material removal are those related to tool speed. In the case of a tool to part system, these are the rotational speed of the tool and the translational speed (feed rate) following the trajectory over the workpiece. The design of experiments for aluminium and magnesium is shown in Table 2.

### Tool footprint measurement

Regarding the tool footprint prediction during finishing process, some previous researches were made in robotic-assisted polishing, also some researches focused on laser polishing, water jet finishing or belt-based grinding. Even material removal prediction is important in cases of stone finishing,<sup>52,53</sup> that is one of the main application industries of finishing technologies, but the importance of this prediction is also shown in the interest of finishing commercial machines' manufacturers, as the case of Zeeko, in order to support the finishing process and implement process control instruments in their finishing machines. In our case, the

intention is to predict the tool footprint for a robotic-assisted mechanical finishing process. To reach this objective, once the probes are polished, the footprint of the tool is measured in a confocal displacement metre (CdM) machine. Polishing process removes a small amount of material so that several passes were made in the same line. The depth of the tool footprint is increased this way in order to make the footprint visible for the CdM machine. Tool footprint in length direction (direction of the robot trajectory) is constant so only the cross section must be analysed. Figure 2(a) shows dimensional measuring process and Figure 2(b) an example of measurement.

Each probe is measured in several cross sections. Data obtained from the collaborative decision-making (CDM) software have to be post-processed. Each footprint has to be extracted, its graph has to be centred and inclination and deformation of the top surface of the probe has to be compensated. Figure 3 shows the tool footprint representation for several polishing conditions. Tool footprint covers a 30-mm length in  $x$  direction, corresponding to the diameter of the tool.

### Tool footprint depth model

The main objective of the research is to characterise the tool footprint that the abrasive tool produces on the workpiece surface. First step is the development of a model for the maximum depth. For this reason, the maximum depth value is related to the polishing

**Table 2.** List of test parameters.

Material	ALU 5083	ALU 5083	ALU 5083	ALU 5083	ALU 5083	ALU 5083	ALU 5083	ALU 5083	ALU 5083	ALU 5083	ALU 5083	ALU 5083	ALU 5083
Abrasive	80	80	80	80	80	80	80	80	80	80	80	80	80
Rotational speed (r/min)	500	500	500	500	500	500	500	500	500	500	500	500	500
Feed rate (mm/min)	30	60	120	180	300	300	300	300	300	300	300	300	300
Probe code	1,2	1,1	1,3	1,4	1,5	1,1,1	1,1,1	1,1,1	1,1,1	1,1,1	1,1,1	1,1,1	1,1,1
Material	ALU 5083	ALU 5083	ALU 5083	ALU 5083	ALU 5083	ALU 5083	ALU 5083	ALU 5083	ALU 5083	ALU 5083	ALU 5083	ALU 5083	ALU 5083
Abrasive	80	80	80	80	80	80	80	80	80	80	80	80	80
Rotational speed (r/min)	1000	1000	2000	2000	2000	2000	2000	2000	2000	2000	2000	2000	2500
Feed rate (mm/min)	180	300	30	60	120	180	180	180	300	300	300	300	50
Probe code	1,8	1,9	1,10	1,11	1,12	1,1	2,1	2,1	2,2	2,2	2,2	2,2	1,1,2
Material	ALU 5083	ALU 5083	ALU 5083	ALU 5083	ALU 5083	ALU 5083	ALU 5083	ALU 5083	ALU 5083	ALU 5083	ALU 5083	ALU 5083	ALU 5083
Abrasive	80	80	80	80	80	80	80	80	80	80	80	80	80
Rotational speed (r/min)	3000	3000	3000	3000	3000	3000	3000	3000	3000	3000	3000	3000	4000
Feed rate (mm/min)	30	60	120	180	300	300	300	300	300	300	300	300	120
Probe code	2,3	2,4	2,5	2,6	2,7	2,8	2,8	2,8	2,9	2,9	2,9	2,9	2,11
Material	ALU 5083	ALU 5083	ALU 5083	ALU 5083	ALU 5083	ALU 5083	ALU 5083	ALU 5083	ALU 5083	ALU 5083	ALU 5083	ALU 5083	ALU 5083
Abrasive	80	80	80	80	80	80	80	80	80	80	80	80	120
Rotational speed (r/min)	4000	5000	5000	6000	6000	6000	6000	6000	6000	6000	6000	6000	8000
Feed rate (mm/min)	300	50	100	12,000	12,000	12,000	12,000	12,000	12,000	12,000	12,000	12,000	6000
Probe code	2,12	1,1,3	1,1,6	1,1,11	1,1,12	1,1,12	1,1,12	1,1,12	1,1,12	1,1,12	1,1,12	1,1,12	1,1,12
Material	ALU 5083	ALU 5083	ALU 5083	ALU 5083	ALU 5083	ALU 5083	ALU 5083	ALU 5083	ALU 5083	ALU 5083	ALU 5083	ALU 5083	ALU 5083
Abrasive	220	220	220	220	220	220	220	220	220	220	220	220	80
Rotational speed (r/min)	1000	1000	2500	2500	5000	5000	5000	5000	5000	5000	5000	5000	4000
Feed rate (mm/min)	50	100	50	100	100	100	100	100	100	100	100	100	4000
Probe code	1,1,7	1,1,10	1,1,8	1,1,11	1,1,12	1,1,12	1,1,12	1,1,12	1,1,12	1,1,12	1,1,12	1,1,12	1,1,12
Material	MAGNESIO	MAGNESIO	MAGNESIO	MAGNESIO	MAGNESIO	MAGNESIO	MAGNESIO	MAGNESIO	MAGNESIO	MAGNESIO	MAGNESIO	MAGNESIO	MAGNESIO
Abrasive	80	80	80	80	80	80	80	80	80	80	80	80	120
Rotational speed (r/min)	6000	6000	6000	6000	6000	6000	6000	6000	6000	6000	6000	6000	6000
Feed rate (mm/min)	12,000	12,000	12,000	12,000	12,000	12,000	12,000	12,000	12,000	12,000	12,000	12,000	12,000
Probe code	14072101_A	14072101_B	14072101_C	14072102_A	14072102_B	14072102_C	14072102_C	14072102_C	14072104_B	14072104_B	14072104_C	14072104_C	14072105_A
Material	MAGNESIO	MAGNESIO	MAGNESIO	MAGNESIO	MAGNESIO	MAGNESIO	MAGNESIO	MAGNESIO	MAGNESIO	MAGNESIO	MAGNESIO	MAGNESIO	MAGNESIO
Abrasive	120	120	120	220	220	220	220	220	220	220	220	220	400
Rotational speed (r/min)	6000	6000	6000	6000	6000	6000	6000	6000	6000	6000	6000	6000	8000
Feed rate (mm/min)	6000	6000	6000	6000	6000	6000	6000	6000	6000	6000	6000	6000	8000
Probe code	14072105_B	14072105_C	14072106_A	14072106_B	14072106_C	14072106_C	14072106_C	14072106_C	14072107_B	14072107_B	14072107_C	14072107_C	14072107_C

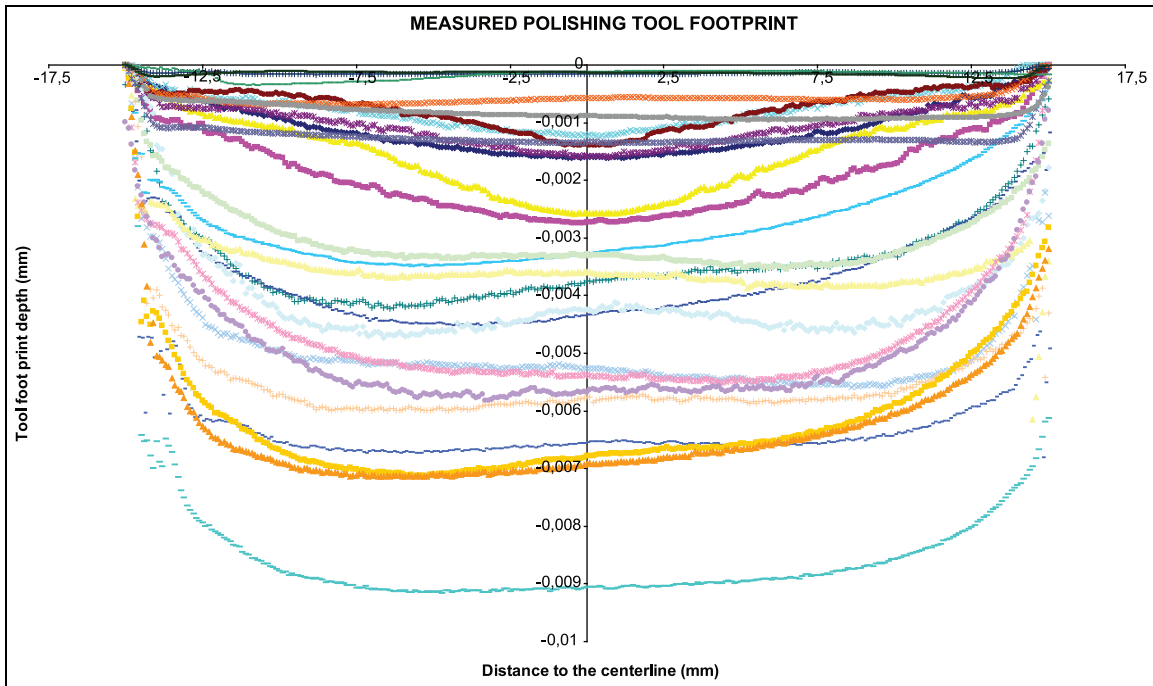


Figure 3. Tool footprint measurements.

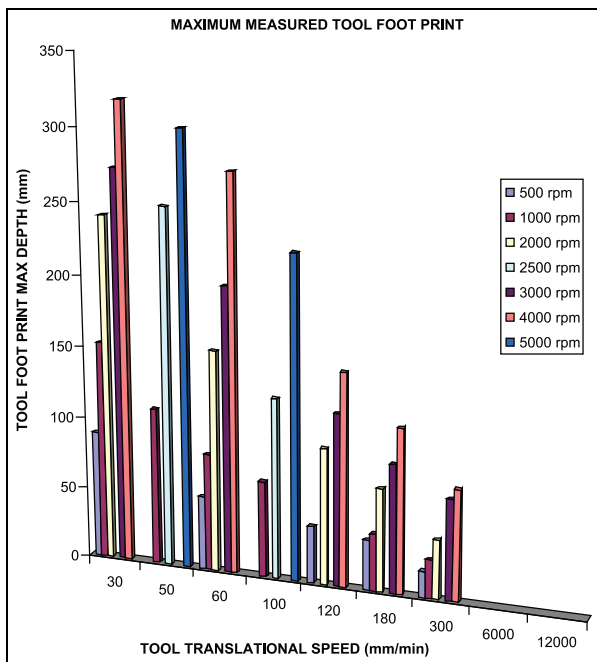


Figure 4. Maximum measured tool footprint values.

parameters. The following methodology is the analysis of all the probes with F80 abrasive polishing aluminium 5083 material. Figure 4 shows the results for different translational and rotational speeds of the tool.

The analysis of the data obtained shows an exponential behaviour. The mathematical model that fits with

Table 3. Parameter 'a' values for the maximum footprint depth depending on tool rotational speed.

Tool rotational speed (r/min)	500	1000	2000	3000	4000
<i>a</i>	759	1240	2023	2438	3010

the results then is an exponential curve that can be expressed as

$$\max \text{ t.f.p. depth} = \frac{a}{x^b} \quad (1)$$

In the case studied for F80 abrasive and aluminium 5083, 'b' fitted value is constant and equal to 0.631. Table 3 shows 'a' values for different tool rotational speeds.

Based on the model obtained, Figure 5 shows the actual values measured on the probes and the theoretical mathematical exponential curve that best fits them.

Figure 6 represents the evolution of parameter 'a' with tool rotational speed revealing a logarithmic behaviour tendency.

The curve fit of the 'a' coefficient values obtained can be mathematically expressed as

$$a = 993.11 \ln(\text{rpm}) - 5503.5 \quad (2)$$

where 'rpm' is the tool translational speed in r/min.

Then, the maximum tool footprint depth can be modelled in function of the polishing technological parameters

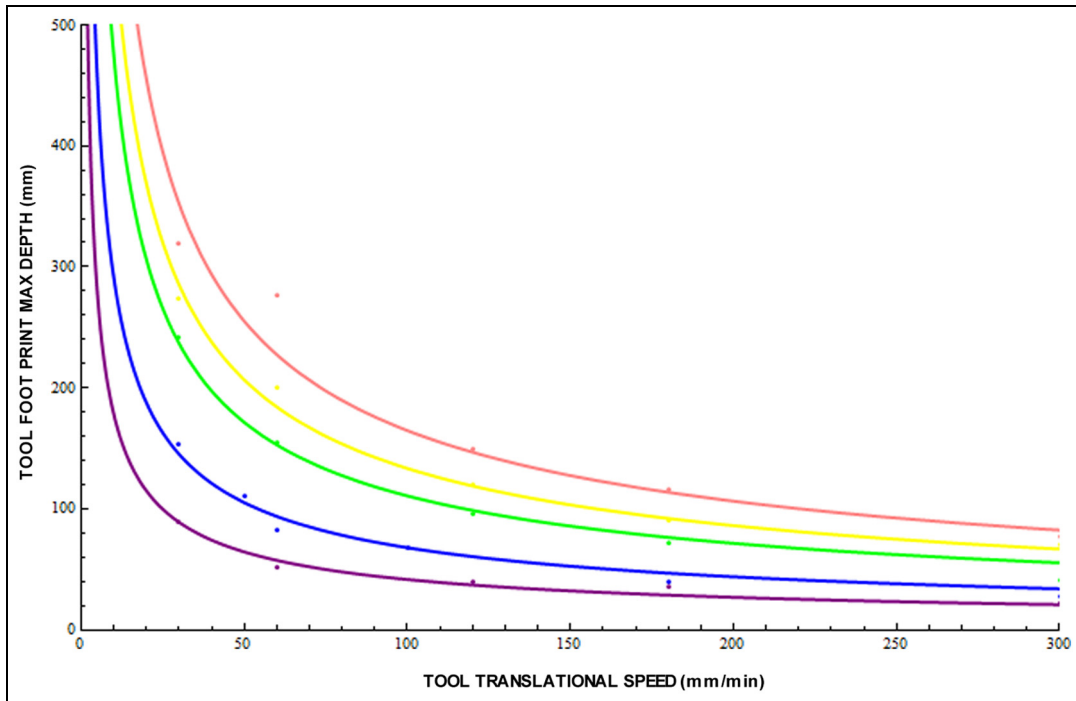


Figure 5. Modelled maximum tool footprint and measured values.

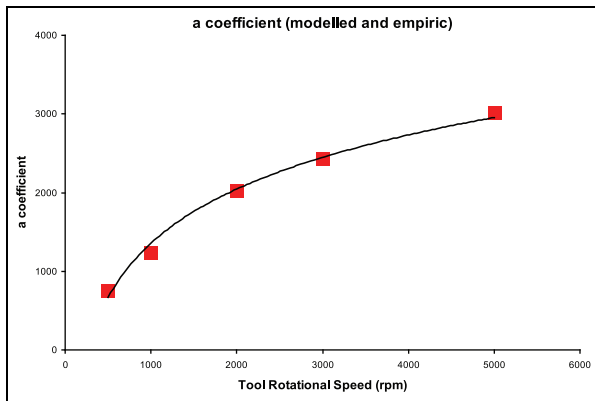


Figure 6. ‘a’ coefficient values for the minimum value of the tool footprint.

$$\max \text{ t.f.p. depth} = \frac{993.11 \ln(\text{rpm}) - 5503.5}{\text{feedrate}^{0.631}} \quad (3)$$

where rpm is the tool rotational speed (r/min), feed rate is the tool translational speed (mm/min) and average error of the maximum tool footprint depth mathematical model is under 5%.

In order to model the whole curve of the tool footprint, the same methodology is used for the mean value of the footprint depth. A constant value for ‘b’ parameter is obtained ( $b = 0.687$ ). Table 4 shows the values for parameter ‘a’ and Figure 7 its graphical representation and logarithmic tendency.

Table 4. Parameter ‘a’ values for the mean footprint depth depending on tool rotational speed.

Tool rotational speed (r/min)	500	1000	2000	3000	4000
a	646	1196	1769	2278	2840

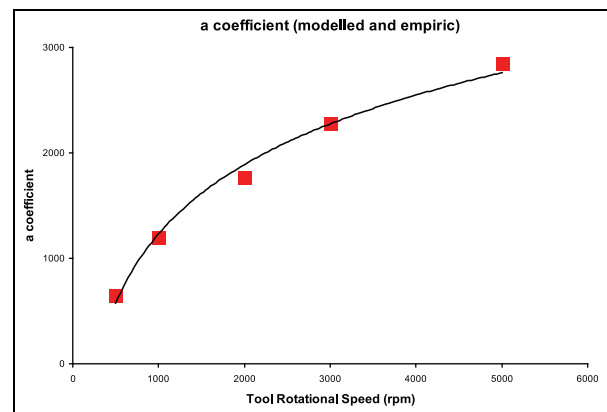


Figure 7. ‘a’ coefficient values for the mean minimum value of the tool footprint.

The mathematical expressions for ‘a’ and mean tool footprint depths are

$$a = 949.41 \ln(\text{rpm}) - 5326.3 \quad (4)$$

**Table 5.** Maximum and mean tool footprint values for several materials and abrasives.

	Rotational speed (r/min)	Translational speed (mm/min)	ALU 5083	ALU 5083	Mg	Mg	Mg	Mg
			F80	F120	F80	F120	F220	F400
Maximum t.f.p. depth ( $\mu\text{m}$ )	6000	12,000	1.61	1.23	6.14	4.09	0.69	0.16
	6000	6000	2.75	1.59	6.80	4.54	1.35	0.35
	8000	6000	2.58	1.40	9.16	6.11	0.96	0.24
Mean t.f.p. depth ( $\mu\text{m}$ )	6000	12,000	1.09	0.75	3.52	2.35	0.57	0.14
	6000	6000	1.91	1.04	6.28	4.19	1.24	0.17
	8000	6000	1.51	0.75	8.48	5.66	0.82	0.15

t.f.p.: total footprint.

$$\text{mean\_t.f.p. depth} = \frac{949.41 \ln(\text{rpm}) - 5326.3}{\text{feedrate}^{0.687}} \quad (5)$$

Average error of the mean maximum tool footprint depth mathematical model is under 5%.

### Tool footprint depth model generalisation for other abrasives and materials

The mathematical model developed permits to express maximum and mean tool depth values as functions of the parameters programmed as the input in the robotic polishing process. These parameters are related to tool speed and rotational and translational movements. This mathematical model is based on the data obtained for a specific material, AL5083, and a specific abrasive, F80.

In order to generalise and extrapolate results for other materials and abrasives, 'material' and 'abrasive' coefficients ('MAT' and 'ABR') are introduced to adapt the mathematical model. Table 5 shows the results obtained for several combinations of workpiece materials and abrasives for maximum and mean values of the tool footprint depth.

Based on the results shown in Table 5 and additional results for Steel F114, the correction coefficients are calculated including material ('MAT'), abrasive ('ABR') and roughness ('Ra') effects. During this research, 65% of the tests were made on AL5083 material. This amount of trials also increased by tests performed during previous phases,<sup>46,48</sup> provides the authors a significant amount of results, so AL5083 is used as reference when defining the 'MAT' coefficient. Regarding 'ABR' coefficient, F80 has been broadly used in previous tests because tool footprint obtained is deeper and easier to be measured than in less rough abrasives. During this research in 70% of the tests, this abrasive was used, so it was set as reference abrasive when determining 'ABR' coefficient. Results are shown in Tables 6–8 for 'MAT', 'ABR' and 'Ra' coefficients, respectively.

Finally, it is necessary to perform a little correction due to the fuzzy oscillations (Figure 8) of the footprint curve derived from the roughness of the surface.

**Table 6.** 'MAT' coefficient for several materials.

Material	'MAT' coefficient
ALU 5083	1
Mg	1.54
Steel F114	0.021

MAT: material.

**Table 7.** 'ABR' coefficient for several abrasives.

Abrasive code	'ABR' coefficient
F80	1
F120	0.81
F220	0.247
F400	0.107

ABR: abrasive.

**Table 8.** Ra coefficient for several abrasives.

Abrasive code	Ra coefficient
F80	3.53
F120	3.35
F220	1.24
F400	0.64

Ra: roughness.

Then taking into account abrasive and material conditions, tool footprint depth equations are as follows

$$\begin{aligned} \text{max t.f.p. depth} &= \text{MAT} \times \text{ABR} \\ &\times \frac{993.11 \ln(\text{rpm}) - 5503.5}{\text{feedrate}^{0.631}} - 2 \times \text{Ra} \end{aligned} \quad (6)$$

$$\begin{aligned} \text{mean t.f.p. depth} &= \text{MAT} \times \text{ABR} \\ &\times \frac{949.41 \ln(\text{rpm}) - 5326.3}{\text{feedrate}^{0.687}} - \text{Ra} \end{aligned} \quad (7)$$

Mathematical model obtained has been compared with the 64 tests performed, and average deviation is under 25%.



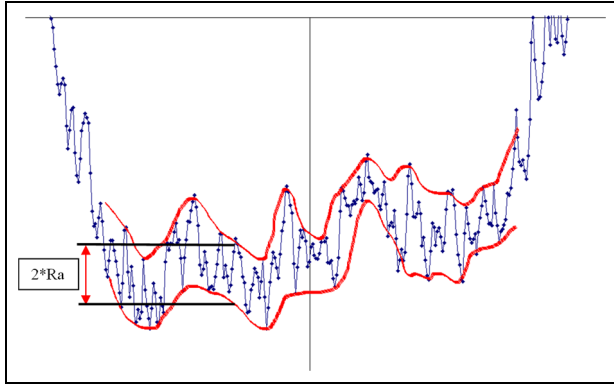


**Figure 8.** Typical measured tool footprint.

**Tool footprint depth cross section model definition**

Once determined the mathematical model that defines the maximum tool print depth for several materials and abrasives in function of the polishing conditions, a further step is to model the shape of the full cross section of the tool footprint. As it was stated in the previous sections, polishing pressure is not considered. This is one of the parameters that would affect the footprint,

conditions, which in fact are the components of a combined movement (translational and rotational) as represented in Figure 9. Figure 9 shows both movements of the tool, rotational in Figure 9(a) and translational due to the robot movement in Figure 9(b). One point in the workpiece that is located at a distance  $y_1$  from the centre line of the robot toolpath shows an absolute speed with two components  $V_r$  and  $V_t$ . These can be translated to a Cartesian coordinate system

$$v_x = \left( \frac{2\pi \cdot \text{rpm} \sqrt{x^2 + y^2}}{60} \right) \cdot \text{Sin} \left( \text{Arctg} \left( \frac{y}{x} \right) \right) + \frac{\text{feed rate}}{60} \tag{8}$$

$$v_y = \left( \frac{2\pi \cdot \text{rpm} \sqrt{x^2 + y^2}}{60} \right) \cdot \text{Cos} \left( \text{Arctg} \left( \frac{y}{x} \right) \right) \tag{9}$$

$$v = \sqrt{v_x^2 + v_y^2} \tag{10}$$

where feed rate is the translational speed (speed of the robot moving on the workpiece) (mm/min) and rpm is the tool rotational speed (r/min).

Simplifying the expression

$$v = \sqrt{\left( \frac{\text{feed rate}}{60} - \frac{\pi \cdot \text{rpm} \cdot \sqrt{x^2 + y^2} \cdot \text{Abs} \left( \frac{y}{x \sqrt{1 + \frac{y^2}{x^2}}} \right)}{30 \cdot \text{Abs}(y)} \right)^2 + \frac{\pi^2 \cdot \text{rpm}^2 \cdot (x^2 + y^2)}{900 \cdot \text{Abs} \left( 1 + \frac{y^2}{x^2} \right)}} \tag{11}$$

but the tool design keeps this value nearly constant if conditions of the robot trajectory allow the interference to remain within the range cited in Section ‘Materials and installation’.

The main parameters that will affect the shape of the curve are tool speed parameters and robot speed

In order to analyse the amount of material removed, that is the focus of this point of the research, not only instant speeds are considered, it is necessary to define the amount of time that any particular point of the workpiece is suffering this speed. As consequence, an integration of the speed is made in function of the time.

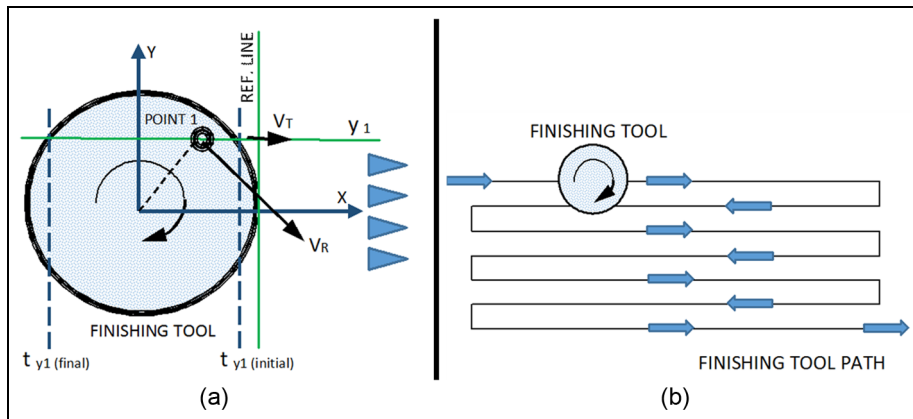


**Figure 9.** Speed schema of the contact between one point in the tool and one point in the workpiece: (a) tool kinematics and (b) finishing tool path.

Next function incorporates the time as variable in the equation

$$x = \frac{-\text{feed rate}}{60} \cdot t + R_{\text{tool}} \quad (12)$$

$v(t) =$

$$\sqrt{\left(\frac{\text{feed rate}}{60} - \frac{1}{30} \pi \cdot \text{rpm} \cdot y \sqrt{\left(R_{\text{tool}} - \frac{\text{feed rate} \cdot t}{60}\right)^2 + y^2} \cdot \text{Abs}\left(\frac{1}{\left(R_{\text{tool}} - \frac{\text{feed rate} \cdot t}{60}\right) \sqrt{1 + \frac{y^2}{\left(R_{\text{tool}} - \frac{\text{feed rate} \cdot t}{60}\right)^2}}\right)\right)^2 + \frac{\pi^2 \cdot \text{rpm}^2 \cdot (-60R_{\text{tool}} + \text{feed rate} \cdot t)^2 \cdot \text{Sign}\left(1 + \frac{y^2}{\left(R_{\text{tool}} - \frac{\text{feed rate} \cdot t}{60}\right)^2}\right)}{324,000}} \quad (13)$$

The objective is to define the cross section of the footprint. Tool footprint cross section represents values for a  $y_i$  point, when  $y_i$  goes from ‘- Radius’ of the tool ( $-R_{\text{tool}}$ ) to ‘+ Radius’ of the tool ( $+R_{\text{tool}}$ ).

For this point of the cross section, located at a distance  $y_i$  from the centre line, integration has to be made from the time instant when tool starts to polish this point  $t_{y_i(\text{initial})}$  to the time instant that tool finishes polishing this point  $t_{y_i(\text{final})}$ .

To determine limit values for the integration, it is necessary to calculate  $t_{y_i(\text{initial})}$  and  $t_{y_i(\text{final})}$ , by solving the equation that represents the geometry of the tool (a circumference) and the line  $y_i$

$$\frac{60 \cdot \text{Abs}(y_i)}{\text{feed rate}} = \sqrt{\left(\frac{R_{\text{tool}} \cdot 60}{\text{feed rate}}\right)^2 - \left(t_{y_i} - \frac{R_{\text{tool}} \cdot 60}{\text{feed rate}}\right)^2} \quad (14)$$

$t_{y_i}$  has two different solutions that correspond to  $t_{y_i(\text{initial})}$  and  $t_{y_i(\text{final})}$ .

Once defined the limits of the integration, the model for the cross section of the tool footprint depth can be described as

From  $y_i = -R_{\text{tool}}$  to  $t_{y_i} = +R_{\text{tool}}$

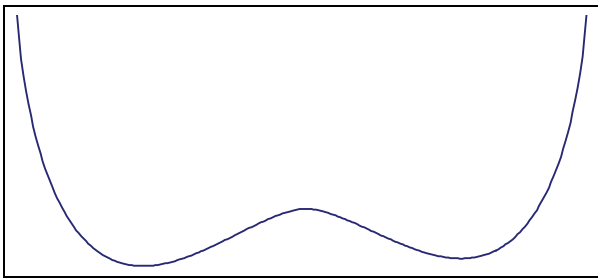


Figure 10. Tool footprint cross section obtained from the model developed.

$$\text{t.f.p. depth}_{y_i} = \int_{t_{y_i(\text{initial})}}^{t_{y_i(\text{final})}} v(t) \quad (15)$$

Figure 10 shows the curve obtained from the model developed.

### Tool footprint depth cross section model adjustment

Typical shape obtained from the model developed fits roughly with the actual shape obtained from the probe trials performed. The reason is that it is necessary to include a correction coefficient that balances the weight assigned to the translational and rotational speeds.

Hocheng et al.<sup>54</sup> analysed the non-uniformity in CMP finishing and concluded that it is majorly determined by the ratio between carrier speed and platen speed, which in the case of robotic mechanic tool to part finishing could be identified as rotational and translational speed of the tool. They described an index that described the kinematic effect in non-uniformity.

During this research, this coefficient is going to be called ‘speed factor’ and will modify the equation of the component of the speed in translational direction (direction of the robot movement) such a way  $v_x$  equation will be as follows

$$v_x = \left(\frac{2\pi \cdot \text{rpm} \sqrt{x^2 + y^2}}{60}\right) \cdot \text{Sin}\left(\text{Arctg}\left(\frac{y}{x}\right)\right) + \text{speed factor} \cdot \frac{\text{feed rate}}{60} \quad (16)$$

‘Speed factor’ will magnify or dwarf the rotational versus translational influence. Figure 11 shows several simulations of the cross section tool footprint for different values of ‘speed factor’.

Now it is possible to fit ‘speed factor’ depending on the polishing parameters (feed rate and tool rotation speed)

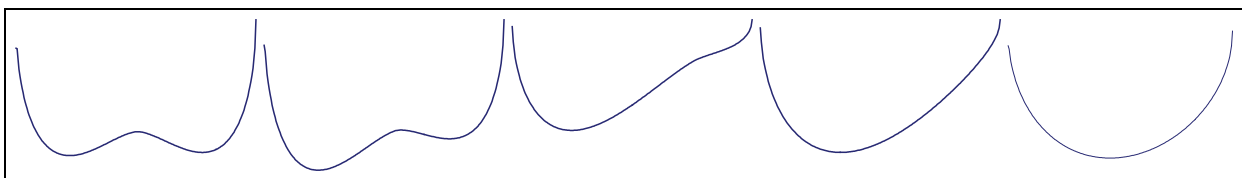
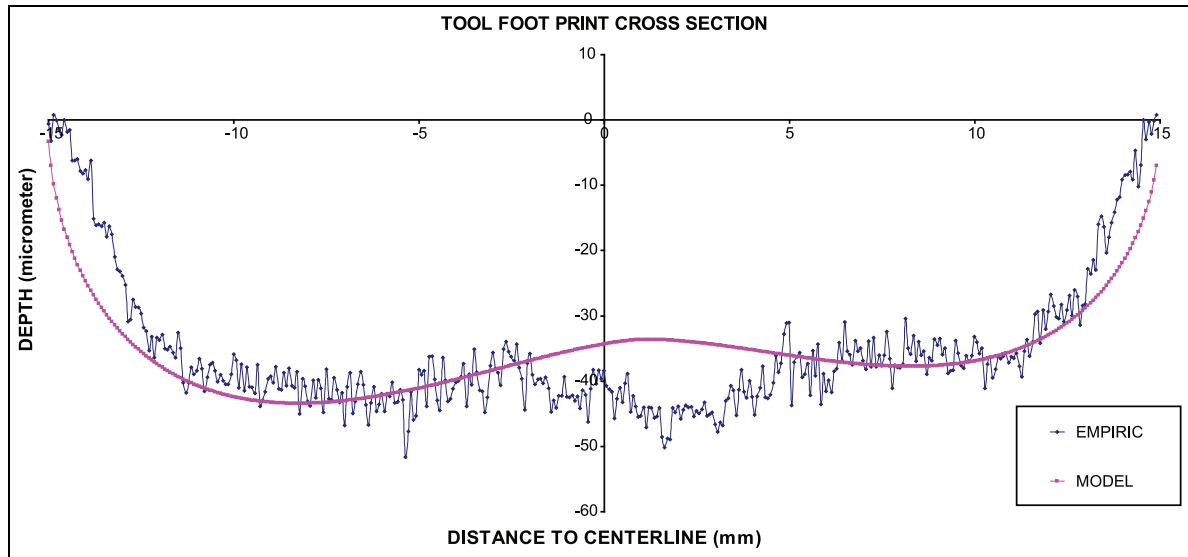


Figure 11. Tool footprint cross section for different ‘speed factor’ values.



**Figure 12.** Polishing parameters modelled and measured tool footprint cross section.

Example 1: material = ALU 5083, abrasive = F80, rpm = 500 r/min and feed rate = 120 mm/min.

$$\text{speed factor} = 4.6745 \cdot e^{0.1091 \cdot \frac{\text{rpm}}{1000 \cdot \text{feed rate}}} \quad (17)$$

### Tool footprint depth cross section model simulator

The finalisation of the model will integrate all the developments in previous sections:

- Mathematical model for the minimum value of the tool footprint depth;
- Mathematical model for the cross section of the tool footprint;
- Corrections with 'speed factor'.

This integration describes the complete mathematical model of the cross section of the tool footprint. To achieve this objective, all the models are included in new software. In the programme, first part is the parameter declaration, where user is required to define material, abrasive code, rotational tool speed, tool diameter and robot translational speed.

Moreover, in this section, coefficients such as 'ABR' and 'MAT' are defined in function of the user selection.

Then, 'speed factor', 'maximum tool footprint depth' and 'mean tool footprint depth' are calculated. Speed factor determines the shape of the graph, taking into account the non-uniformity of the section obtained derived from the rotational and translational speed of the tool.

After this point, the calculations based on the methodology developed in the research will run based on the mathematical model, and it will be scaled in function of the 'max t.f.p. depth', obtained from the algorithm execution. 'Mean t.f.p. depth' is used to check the scale obtained from the 'max t.f.p. depth' value calculated. The output from the software will be the tool

footprint section graph predicted for the parameters and values of the specific finishing task.

We can compare the results obtained from the software with the measured data obtained during the trials. Figures 12–15 compare the model with the actual empiric data for several input conditions.

## Conclusion

The aim of this research was to tackle the question of developing a technological base to improve the polishing process. It is a fact that cannot be ignored that as a consequence of traditional, manually made finishing process currently performed in the companies, a series of quality problems remain in the present days. These are derived from the lack of control process. Specifically, there is not control on the amount of material removed and the quality of the final surfaces. Even in current process, most of the quality thresholds depend on the subjective criteria of a skilled worker.

The issue under consideration can be summed up as the fact that during this investigation a 'tool to part', automated polishing process based on industrial robotic is demonstrated as a suitable manufacturing system to automate this finishing task.

A complex mathematical model has been developed that uses as input the technological polishing parameters such as tool rotational speed, robot translational speed and variables related to polished material and abrasive to be used. The model generates as output a prediction of the tool footprint cross section graph.

The model developed has been programmed in a software in order to automate the tool footprint prediction.

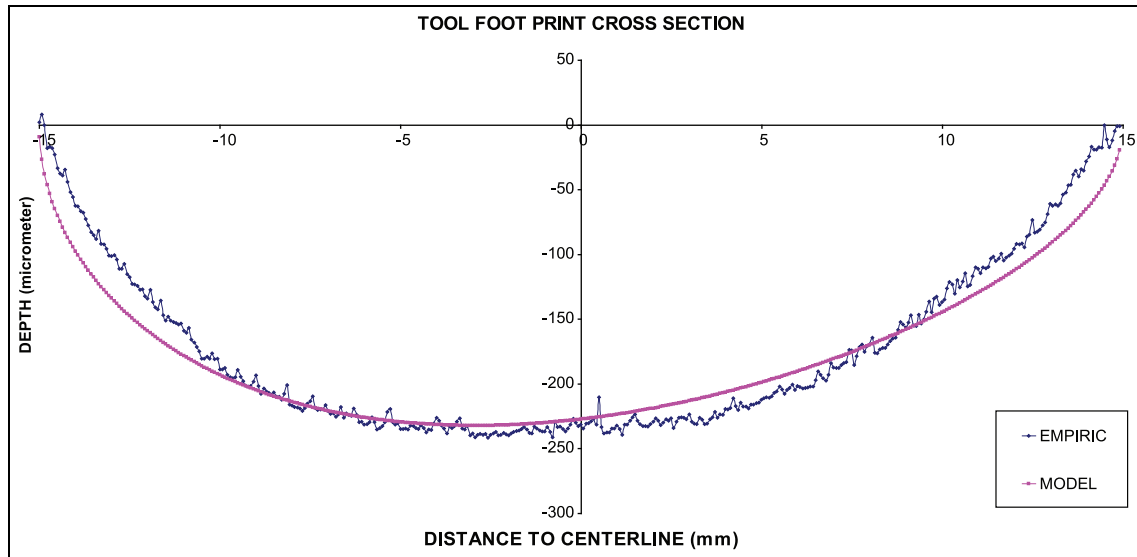


**Figure 13.** Polishing parameters modelled and measured tool footprint cross section.  
Example 2: material = ALU 5083, abrasive = F80, rpm = 2000 r/min and feed rate = 30 mm/min.

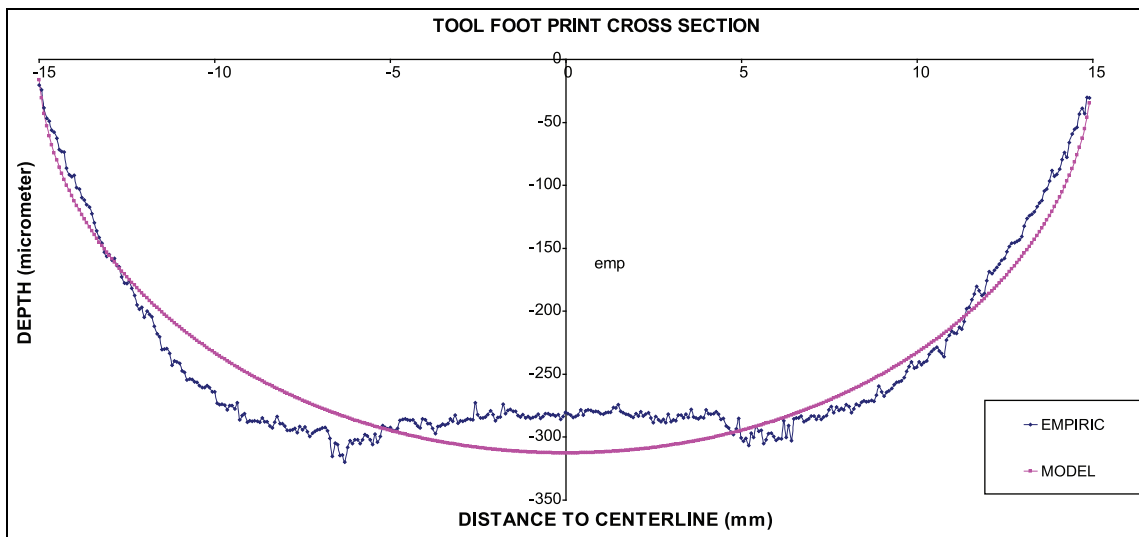


**Figure 14.** Polishing parameters modelled and measured tool footprint cross section.  
Example 3: material = ALU 5083, abrasive = F80, rpm = 4000 r/min and feed rate = 30 mm/min.

The results of the model have been compared with the experimental trials performed in different metallic alloys such as aluminium 5083, magnesium alloy and steel F114 (for several abrasive grain sizes (P80, P120, P220 and P400), with a rotational tool speed in the range of 500–8000 r/min with a 30- to 50-mm-diameter tool, and translational tool speed in the range of 30–12,000 mm/min). Maximum absolute deviations between the model and the empiric results remain under 25% in the worst cases and under 15% in most of them.

Model developed is a grant to implement robot ‘tool to part’ polishing in industrial environments and industrial applications.

Moreover, the accuracy in the prediction of the amount of material removed by the abrasive can set the base for a ‘conformal polishing’ concept. This means not to use polishing process exclusively as a surface finishing task, but also as a new predictable manufacturing process. It will allow removal of a very small amount of material through a controlled way. This concept could be applied in the near future to correct

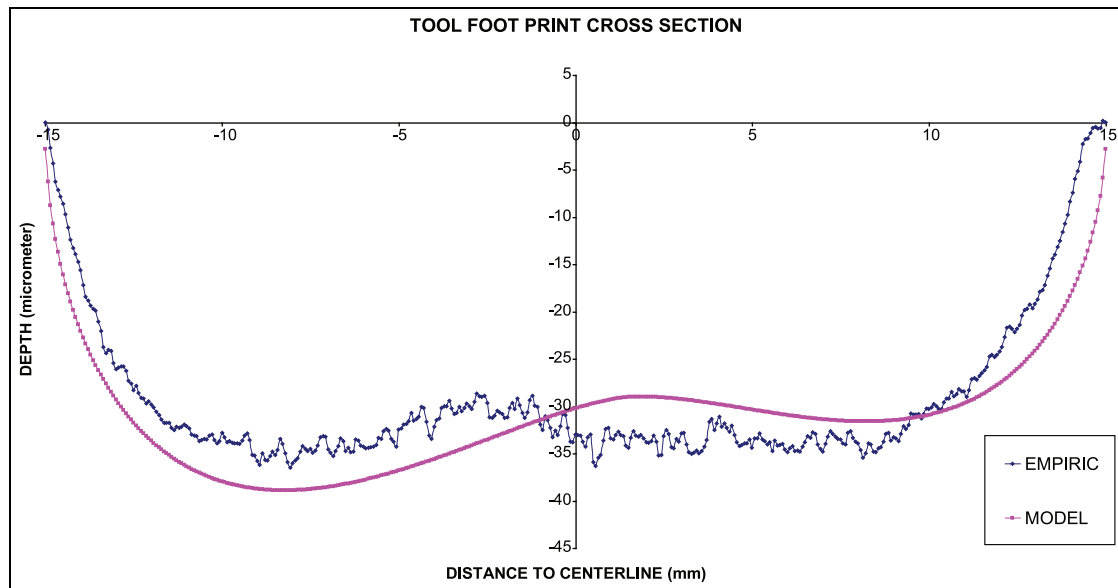


**Figure 15.** Polishing parameters modelled and measured tool footprint cross section.

Example 4: material = ALU 5083, abrasive = F220, rpm = 1000 r/min and feed rate = 50 mm/min.

shape deviations in metallic parts or even to make a part fit a programmed shape.

### Declaration of conflicting interests

The author(s) declared no potential conflicts of interest with respect to the research, authorship and/or publication of this article.

### Funding

The author(s) received no financial support for the research, authorship and/or publication of this article.

### References

- Shi FB and Zhao B. Modelling of chemical-mechanical polishing with soft pads. *Appl Phys* 1998; 67: 249–252.
- Lin ZC and Ho CY. Analysis and application of grey relation and ANOVA in chemical-mechanical polishing process parameters. *Int J Adv Manuf Tech* 2003; 21: 10–14.
- Lin YY and Lo SP. A study on the stress and uniformity of the wafer surface for the chemical-mechanical polishing process. *Int J Adv Manuf Tech* 2003; 22: 401–409.
- Lin YY and Lo SP. A study of a finite element model for the chemical polishing process. *Int J Adv Manuf Tech* 2004; 23: 644–650.
- Pa PS. Continuous finishing processes using a combination of burnishing and electrochemical finishing on bore surfaces. *Int J Adv Manuf Tech* 2010; 49: 147–154.
- Zeng S and Blunt L. Experimental investigation and analytical modelling of the effects of process parameters on material removal rate for bonnet polishing of cobalt chrome alloy. *Precis Eng* 2014; 38: 348–355.
- Cheung CF, Kong LB, Ho LT, et al. Modelling and simulation of structure surface generation using computer controlled ultra-precision polishing. *Precis Eng* 2011; 35: 574–590.
- Song Y, Liang W and Yang Y. A method for grinding removal control for a robot belt grinding system. *J Intell Manuf* 2012; 23: 1903–1913.
- Wu S, Kazerounian K, Gan Z, et al. A simulation platform for optimal selection of robotic belt system parameters. *Int J Adv Manuf Tech* 2013; 64: 447–458.
- Bambrick S, Bechtold M, DeFisher S, et al. Ogive and freeform polishing with ultraform finishing. In: *Proceedings of SPIE, volume 8016: state-of-the-art in optical finishing*, Orlando, FL, 20 May 2011.
- DeFisher S, Fess E and Wolfs F. Freeform and conformal optical manufacturing. In: *Proceedings of SPIE, volume 8708: metrology and finishing of flat, free-form, and conformal optics*, Baltimore, MD, 4 June 2013.
- Fess E and DeFisher S. Advancements in asphere manufacturing. In: *Proceedings of SPIE, volume 8838: optical manufacturing I*, San Diego, CA, 7 September 2013.
- Kordonski WI and Jacobs SD. Magnetorheological finishing. *Int J Modern Phys B* 1996; 10: 2837–2848.
- Kordonski WI and Golini D. Fundamentals of magnetorheological fluid utilization in high precision finishing. *J Intell Mater Syst* 1999; 10: 683–689.
- Walker DD, Beaucamp ATH, Brooks D, et al. New results from the precessions polishing process scaled to larger sizes. In: *Proceedings of SPIE, volume 5494: astronomical telescopes and instrumentation meeting*, Glasgow, 24 September 2004, pp.71–80.
- Walker DD, Freeman R, Hobbs G, et al. Zeeko 1 metre polishing system. In: *Proceedings of the 7th international conference on Lamdamap*, Cranfield, 24 June–1 July 2005, p.240.
- Narayanasamy R, Ramesh T and Pandey KS. An experimental investigation on strain hardening behaviour of aluminium–3.5% alumina powder metallurgy composite perform under various stress states during cold upset forming. *Mater Design* 2007; 28: 1211–1223.

18. Li Y, Gracewski SM, Funkebusch PD, et al. Analysis of chatter in contour grinding of optical materials. *Int J Mach Tool Manu* 2002; 42: 1095–1103.
19. Sachtleber M, Raabe D and Weiland H. Surface roughening and colour changes of coated aluminium sheets during plastic straining. *J Mater Process Tech* 2004; 148: 68–76.
20. Xhang X, Krewet C and Kuhlenko B. Automatic classification of defects on the product surface in grinding and polishing. *Int J Mach Tool Manu* 2006; 46: 59–69.
21. Márquez JJ, Pérez JM, Ríos J, et al. Process modelling for robotic polishing. *J Mater Process Tech* 2005; 159: 69–82.
22. Chaves-Jacob J, Linares JM and Sprauel JM. Improving tool wear and surface covering in polishing via toolpath optimization. *J Mater Process Tech* 2013; 213: 1661–1668.
23. Chen CH, Ch A, Juang YS, et al. Generation of fractal toolpaths for irregular shapes of surface finishing areas. *J Mater Process Tech* 2002; 127: 146–150.
24. Lee MC, Go SJ, Jun CS, et al. A robust trajectory tracking control of a polishing robot system based on CAM data. *Robot Comput Integr Manuf* 2001; 17: 177–183.
25. Tam HY, Lui O, Ch H, et al. Robotic polishing of free-form surfaces using scanning paths. *J Mater Process Tech* 1999; 95: 191–200.
26. Huisson JP, Ismail F, Jafari F, et al. Automated polishing of die steel surfaces. *Int J Adv Manuf Tech* 2002; 19: 285–290.
27. Pessoles X and Tournier CH. Automatic polishing process of plastic injection moulds on a 5-axis milling center. *J Mater Process Tech* 2009; 209: 3665–3673.
28. Feng D, Sun Y and Du H. Investigations on the automatic precision polishing of curved surfaces using a five-axis machining centre. *Int J Adv Manuf Tech* 2014; 72: 1625–1637.
29. Tsai MJ and Huang JF. Efficient automatic polishing process with a new compliant abrasive tool. *Int J Adv Manuf Tech* 2006; 30: 817–827.
30. Tsai MJ, Huang JF and Kao WL. Robotic polishing of precision molds with uniform material removal control. *Int J Mach Tool Manu* 2009; 49: 885–895.
31. Maury A, Ouma D, Boning D, et al. A modification to Preston's equation and impact on pattern density effect modelling. In: *Advance metallization and interconnect system for ULSI application*, San Diego, CA, 23 October 1997.
32. Park KH, Kim HJ, Chang OM, et al. Effects of pad properties on material removal in chemical. *J Mater Process Tech* 2007; 187–188: 73–76.
33. McGrath J and Davis C. Polishing pad surface characterisation in chemical. *J Mater Process Tech* 2004; 153–154: 666–673.
34. Jin XL and Zhang LC. A statistical model for material removal prediction in polishing. *Wear* 2012; 274–275: 203–211.
35. Xin J, Cai W and Tichy JA. A fundamental model proposed for material removal in chemical mechanical polishing. *Wear* 2010; 268: 837–844.
36. Klamecki BE. Comparison of material removal rate models and experimental results for the double-sided polishing process. *J Mater Process Tech* 2001; 109: 248–253.
37. Roswell A, Xi F and Liu G. Modelling and analysis of contact stress for automated polishing. *Int J Mach Tool Manu* 2006; 46: 424–435.
38. Shinhaerl M, Rascher R, Stamp R, et al. Utilisation of time-variant influence functions in the computer controlled polishing. *Precis Eng* 2008; 32: 47–54.
39. Tam HY and Cheng H. An investigation of the effects of the tool path on the removal. *J Mater Process Tech* 2010; 210: 807–818.
40. Klocke F, Brecher C, Zunke R, et al. Corrective polishing of complex ceramics geometries. *Precis Eng* 2011; 35: 258–261.
41. Guo J, Suzuki H, Morita S, et al. A real-time polishing force control system for ultraprecision finishing of micro-optic. *Precis Eng* 2013; 37: 787–792.
42. Zhan J. Study on the manufacturing process controlling for aspheric surface ballonet polishing. *Int J Adv Manuf Tech* 2013; 69: 171–179.
43. Zhan J. An improved polishing method by force controlling and its application in aspheric surfaces ballonet polishing. *Int J Adv Manuf Tech* 2013; 68: 2253–2260.
44. Shi Y, Zheng D, Hu L, et al. NC polishing of aspheric surfaces under control of constant pressure using a magnetorheological torque servo. *Int J Adv Manuf Tech* 2012; 58: 1061–1073.
45. Zhan J and Yu S. Study on error compensation of machining force in aspheric surfaces polishing by profile-adaptive hybrid movement–force control. *Int J Adv Manuf Tech* 2011; 54: 879–885.
46. Dieste JA, Fernández A, Roba D, et al. Automatic grinding and polishing using spherical robot. *Proced Eng* 2013; 63: 938–946.
47. Wu X, Kita Y and Ikoku K. New polishing technology of free form surface by GC. *J Mater Process Tech* 2007; 187–188: 81–84.
48. Dieste JA, Fernández A and Roba D. Rapid finishing of free form surfaces using milling machine and spherical robot. *Adv Sci Lett* 2013; 19: 849–852.
49. FEPA-Standard 42-1:2006. Grains of fused aluminium oxide, silicon carbide and other abrasive materials for bonded abrasives and for general industrial applications Macrogrits F 4 to F 220.
50. ISO 8486. Bonded abrasives – determination and designation of grain size distribution – parts 1 and 2. 2nd ed., 2007.
51. Saito K, Miyoshi T and Sasaki T. Automation of polishing process of a cavity surface on dies and moulds by using an expert system. *CIRP Ann Manuf Techn* 1993; 42: 553–556.
52. Wang G, Wang Y and Xua Z. Modeling and analysis of the material removal depth for stone polishing. *J Mater Process Tech* 2009; 209: 2453–2463.
53. Xia F and Zhou D. Modeling surface roughness in the stone polishing process. *Int J Mach Tool Manu* 2005; 45: 365–372.
54. Hocheng H, Tsai HY and Tsai MS. Effects of kinematic variables on nonuniformity in chemical mechanical planarization. *Int J Mach Tool Manu* 2000; 40: 1651–1669.